A Method for the Time-Varying Nonlinear Prediction of Complex Nonstationary Biomedical Signals

Luca Faes*, *Member, IEEE*, Ki H. Chon, *Senior Member, IEEE*, and Giandomenico Nollo, *Member, IEEE*

***Abstract*—A method to perform time-varying (TV) nonlinear prediction of biomedical signals in the presence of nonstationarity is presented in this paper. The method is based on identification of TV autoregressive models through expansion of the TV coefficients onto a set of basis functions and on k-nearest neighbor local linear approximation to perform nonlinear prediction. The approach provides reasonable nonlinear prediction even for TV deterministic chaotic signals, which has been a daunting task to date. Moreover, the method is used in conjunction with a TV surrogate method to provide statistical validation that the presence of nonlinearity is not due to nonstationarity itself. The approach is tested on simulated linear and nonlinear signals reproducing both time-invariant (TIV) and TV dynamics to assess its ability to quantify TIV and TV degrees of predictability and detect nonlinearity. Applicative examples relevant to heart rate variability and EEG analyses are then illustrated.**

***Index Terms*—Complexity, EEG, heart rate variability (HRV), local nonlinear prediction, nonlinear dynamics, nonstationary signals, surrogate data.**

I. Introduction

DUE TO THE inherent time-varying (TV) characteristics of biological systems, most biomedical signals are expected to be nonstationary, independently of the time scale over which they are analyzed. As an example, heart rate variability (HRV) time series and EEG signals are expected to show TV behaviors in both experimental and clinical recordings [1], [2]. Consequently, a large number of TV algorithms have been developed for the analysis of these signals. Among them, TV linear parametric models offer compactness of the signal representation and high resolution, and have been proposed for HRV and EEG analysis [3], [4]. On the other hand, there is also evidence that biomedical signals very often exhibit time-, state-, and site-dependent degrees of nonlinearity. In fact, many approaches performing nonlinear dynamical analysis of cardiovascular and brain signals have been proposed [5], [6]. However, the reliability of nonlinear measures of complexity is dependent on the validity of the underlying assumption of stationarity, which is difficult to attain in biomedical recordings.

Manuscript received June 18, 2008; revised October 16, 2008. First published November 7, 2008; current version published March 25, 2009. *Asterisk indicates corresponding author.*

*L. Faes is with the Biophysics and Biosignals Laboratory, Department of Physics, University of Trento, Trento 38050, Italy (e-mail: luca.faes@unitn.it).

K. H. Chon is with the Department of Biomedical Engineering, State University of New York, Stony Brook, NY 11794-8181 USA (e-mail: ki.chon@sunysb.edu).

G. Nollo is with the Biophysics and Biosignals Laboratory, Department of Physics, University of Trento, Trento 38050, Italy (e-mail: giandomenico.nollo@unitn.it).

Digital Object Identifier 10.1109/TBME.2008.2008726

This study proposes a new method for the nonlinear analysis of biomedical signals in the presence of nonstationary dynamics. The method performs nonlinear prediction through k-nearest neighbor local linear approximation [7], i.e., defining a linear model whose coefficients are identified from only the k-nearest neighbors of the current state. Moreover, the possible evolution over time of the local linear relationship is accounted for by setting TV model coefficients, according to an expansion onto a set of predefined basis functions [8]. The proposed method appears to be one of the few existing approaches that are able to handle both nonlinear (even deterministic chaotic) and nonstationary dynamics.

This letter is organized as follows. Section II presents the method and describes how it performs nonlinear prediction, as well as detection of nonlinearity, in nonstationary signals. Section III describes its validation, in comparison with time-invariant (TIV) nonlinear prediction, on simulated linear and nonlinear dynamics with imposed stationary or nonstationary behaviors. Section IV describes examples of application to typical HRV and EEG signals. Conclusions are drawn in Section V.

II. TV Nonlinear Prediction

Given a normalized time series y of N samples, its current value $y(n)$ is predicted as a linear combination of the lagged samples forming the reference vector $\mathbf{y}_P(n) = [y(n-\tau), y(n-2\tau), \ldots, y(n-P\tau)]^T$ by means of a linear TV autoregressive (AR) model: $y(n) = \mathbf{a}(n).\mathbf{y}_P(n) + e(n)$, where $e(n)$ is the prediction error and $\mathbf{a}(n) = [a(1,n), \ldots, a(P,n)]$ is the vector of the TV AR coefficients to be determined. Nonlinear prediction is accomplished according to a k-nearest neighbor local linear approximation [7]. Specifically, the k-nearest neighbors of the reference vector $\mathbf{y}_P(n_1), \ldots, \mathbf{y}_P(n_k)$ are found as the k vectors having the minimum Euclidean distance to $\mathbf{y}_P(n)$, and are used to set a system of k equations

$$y(n_j) = \sum_{i=1}^{P} a(i, n_j)\, y(n_j - i\tau), \qquad j = 1, \ldots, k. \quad (1)$$

The system (1) is solved by expanding the TV coefficients onto a set of basis functions π such that

$$a(i,\ n_j) = \sum\nolimits_{m=0}^{M} \alpha(i,\ m)\, \pi_m(n_j) \quad (2)$$

where $\alpha(i, m)$ represent the expansion parameters with $M+1$ as the maximum number of basis sequences [8]. The system resulting after expansion is TIV, as the $P(M+1)$ new coefficients, $\alpha(i,m)$, $i = 1, \ldots, P$, $m = 0, \ldots, M$, are not functions

of time. Hence, it is identified by traditional least-squares optimization, and the estimated coefficients $\hat{\alpha}(i,m)$ are used to predict $y(n)$

$$\hat{y}(n) = \sum_{i=1}^{P} \sum_{m=0}^{M} \hat{\alpha}(i,m)\, \pi_m(n)\, y(n - i\tau). \tag{3}$$

Prediction is performed for each sample of y, and a measure of unpredictability of the series is finally taken as the mean-squared prediction error (MSPE)

$$\text{MSPE} = (N - P\tau)^{-1} \sum_{n=P\tau+1}^{N} (y(n) - \hat{y}(n))^2. \tag{4}$$

The two key parameters that determine how the proposed approach deals with nonlinear and nonstationary dynamics are the number of neighbors k and the number of basis functions M, respectively. Specifically, the use of a low k allows to perform local nonlinear prediction since any possible nonlinear relation between $\mathbf{y}_P(n)$ and $y(n)$ is approximated locally in the P-dimensional state space; by contrast, a high k determines linear AR prediction since a global relationship between $\mathbf{y}_P(n)$ and $y(n)$ is imposed [9]. Hence, nonlinear (even chaotic) dynamics are captured using a local predictor, while linear dynamics can be described either by local or by global predictors. Moreover, nonstationary dynamics can be tracked by defining a TV model with $M \geq 1$, while without basis function expansion $(M = 0, \pi_0(n) = 1)$, a TIV model working only under stationary conditions is defined. In this study, we implemented two different types of basis functions: Legendre polynomials, which are appropriate for smoothly changing dynamics, and Walsh functions, which behave well for dynamics exhibiting fast transients and/or burst-like behaviors [8]. After evaluation of the proper type and number M (via the mean-square-error criterion) of basis functions to be used, the number of neighbors was let free to vary between $k_{\min} = P(M+1)$ and $k_{\max} = N - P\tau - 1$ to allow a comparison between local and global AR models. The embedding parameters were optimized to allow a proper description of the signal under analysis. Specifically, the time lag was set either to $\tau = 1$, to focus on a short temporal scale or at the value corresponding to the autocorrelation function dropping to its $(1/e)$th value, to adapt the temporal scale to the sampling frequency in sampled signals. The AR model order was determined by varying P from 1 to 12 and selecting the value yielding the lowest MSPE.

The proposed approach was used in conjunction with the method of surrogate data [10] to test the presence of nonlinear dynamics in the analyzed signals. Surrogate data to be used for TV nonlinear prediction were generated by the parametric approach, i.e., fitting a TV AR model to the original signal and regressing the estimated TV model coefficients with independent noise realizations to produce the surrogates [11]. The MSPE index was used as nonlinear discriminating statistic, and nonlinearity was detected when the MSPE of the original signal was smaller than the threshold value given by the fifth percentile of the MSPE distribution estimated from 100 surrogate series.

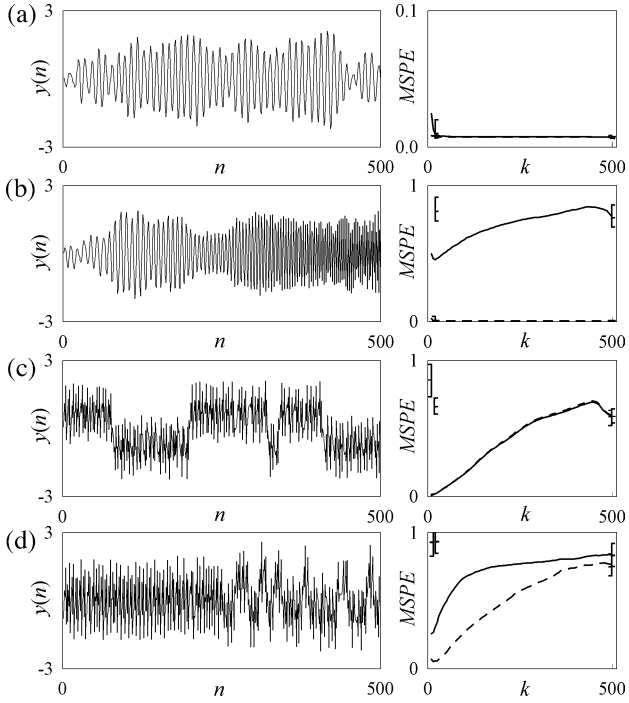

Fig. 1. (a) TIV linear time series. (b) TV linear time series. (c) TIV nonlinear time series. (d) TV nonlinear time series. Right panels show MSPE estimated by TIV prediction ($M = 0$, solid curve) and TV prediction ($M \geq 1$, dashed curve) by varying the number of neighbors k. Distribution bars of MSPE (5th, 50th, and 95th percentiles; right dashes: TIV approach; left dashes: TV approach) estimated from 100 surrogate series are also indicated for local prediction ($k = k_{\min}$) and global prediction ($k = k_{\max}$). MSPE is estimated with $\tau = 1$ and $P = 2$, using $M = 2$ Legendre basis functions in (a) and (b), and $M = 1$ Walsh basis function in (c) and (d).

To provide a comparison with the traditional test for nonlinearity, we also performed TIV nonlinear prediction, implementing TIV AR models ($M = 0$) to estimate MSPE and generate TIV surrogates. The comparison is important because the traditional surrogate-based nonlinearity tests require stationarity [10], and its application to nonstationary signals may lead to erroneous detections of nonlinear dynamics [11].

III. Method Validation

The proposed approach was validated on simulated linear and nonlinear time series, in which either stationary or nonstationary conditions were reproduced. In the first simulation, the ability of the method to quantify the degree of predictability and detect the nature of the dynamics was tested on a linear second-order AR (AR2) process with a narrow-band oscillation at 0.1 Hz, and the nonlinear map described in [12] ($N = 500$). Stationary realizations of the two dynamics are shown in Fig. 1(a) and (c), respectively, while nonstationary behaviors were obtained by imposing a quadratic increase of the frequency of the AR2 process between 0.1 and 0.4 Hz [see Fig. 1(b)] and a step variation (occurring at $n = 250$) of the coefficient controlling the nonlinear dynamics [see Fig. 1(d)]. Results of local linear prediction are expressed in Fig. 1 by plotting the MSPE index as a function of k. During stationary conditions, TIV and TV predictions

gave comparable results, correctly capturing the predictability of the dynamics (very low MSPE) with a global neighborhood (high k) for the linear series [see Fig. 1(a)] and a very local neighborhood (small k) for the nonlinear series [see Fig. 1(c)]. By contrast, the predictability of nonstationary time series was captured only by TV prediction, while the TIV approach gave an erroneous indication of high complexity [high MSPE; Fig. 1(b) and (d)]. Moreover, the linear TV dynamics of Fig. 1(b) was detected erroneously as nonlinear by TIV nonlinear prediction, as the original MSPE values were outside the distribution of the surrogates for local prediction, while the TV approach was used for correct detection.

The second simulation tested the method's ability to follow changes over time by using predictability as a figure of merit. The first signal [see Fig. 2(a)] was a linear AR2 process with main oscillation at 10 Hz (sampling rate = 128 Hz), in which four increasing predictability levels were obtained by step variations in four subsequent time windows of the parameter controlling the regularity of the process. The application to ten realizations of the process evidenced that the MSPE values evaluated within each of the four stationary subsegments were better bounded inside their expected range when the TV method was implemented, while the TIV approach was biased toward a worse prediction [i.e., a higher MSPE; Fig. 2(b)]. The second signal, shown in Fig. 2(c), was the nonlinear map produced by the Mackey–Glass differential equation with temporal parameter $T = 10$, for which 1024 points were taken (sampling rate = 128 Hz) after discarding 1000 points as transients. As shown in Fig. 2(d), the maximum predictability was achieved for a local predictor with $k = 40$, and addition of noise caused a progressive unpredictability of the signal, with MSPE ranging from 0.21 for the clean signal to 0.91 for the 0 dB noise level. To achieve TV predictability degrees, the map was corrupted with additive noise of variance linearly increasing in time up to the 0 dB level. As seen in Fig. 2(e) (average over ten realizations), the MSPE evaluated over time after using TV nonlinear prediction matched with good approximation the expected linear variation in predictability, while TIV prediction was unable to follow the changes in predictability due to progressive noise contamination.

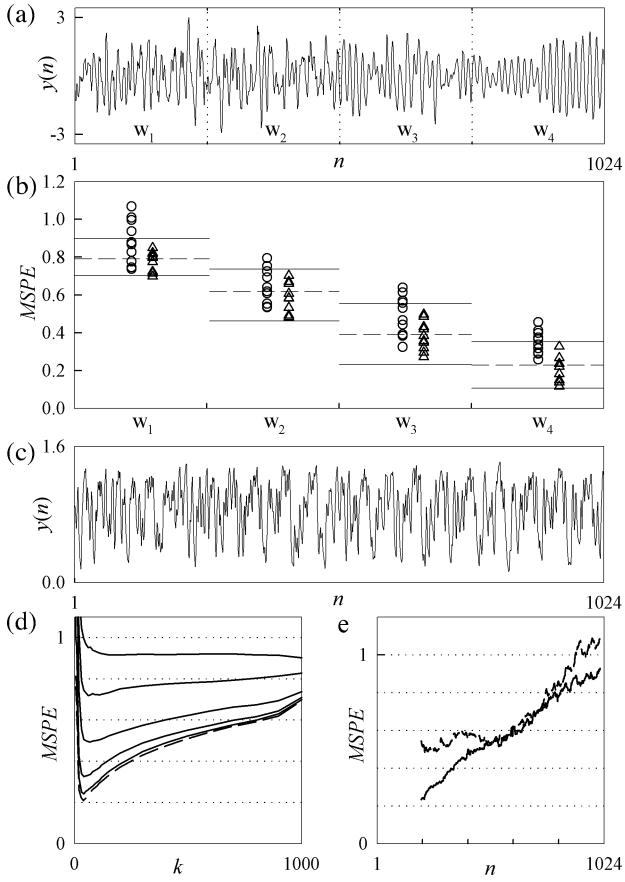

Fig. 2. (a) TV linear AR process. (b) MSPE estimated ($\tau = 3, P = 4$) for ten realizations of the process by TIV prediction ($M = 0$, circles) and TV prediction ($M = 4$ Walsh basis functions, triangles) within each of the four stationary windows (w_1, w_2, w_3, and w_4) of the TV signal. The bound lines indicated within each window are the expected median (dashed) and percentiles (5th and 95th, solid) of MSPE distribution, estimated from 100 stationary segments of 256 points each. (c) Mackey–Glass signal. (d) MSPE estimated for TIV nonlinear prediction ($M = 0, \tau = 3$, and $P = 6$) as a function of the number of neighbors k for the clean Mackey–Glass signal (dashed curve) and after 20, 15, 10, 5, and 0 dB noise addition (solid curves, from bottom to top). (e) Time course of the MSPE index estimated ($\tau = 3, P = 6$) after adding noise with variance linearly increasing in time to the clean map, using both TIV ($M = 0$, upper dashed curve) and TV ($M = 1$ Legendre function, lower solid curve) approaches with $k = 40$. MSPE is calculated over subsegments of 200 samples, sample-by-sample forward-shifted in time.

IV. Illustrative Examples

To demonstrate the usefulness of the proposed TV nonlinear prediction method, we report representative examples of application on HRV time series and EEG signals. It is worth noting that the computational complexity of TV nonlinear prediction, as observed in this application, is compatible with a real-time implementation of the algorithm on biomedical signals.

Fig. 3 illustrates the application to heart period series (RR interval sequences) measured from the ECG in healthy subjects, resting in the supine position either during spontaneous breathing or paced breathing at 0.2 Hz. The series of Fig. 3(a)–(c) were acquired during carefully controlled experimental settings that should guarantee the absence of important transients, while the one in Fig. 3(d) is not stationary as at the beat 200, there was a transition from spontaneous to paced breathing. While for the first series, both TIV and TV predictors detected the dynamics as linear [MSPE was lower for $k = 295$ than for $k = 50$, and original MSPE values were encompassed by their surrogate distribution; Fig. 3(a)], the second series was detected as nonlinear by TIV prediction ($M = 0$) and linear by TV prediction [$M = 2$, Legendre functions; Fig. 3(b)]. This disagreement indicates a possible confounding role of nonstationarity in the detection of nonlinear dynamics performed by the traditional TIV approach [11] and suggests the appropriateness of using a TV approach even in the short-term analysis. The series measured during paced breathing [see Fig. 3(c) and (d)] was detected as nonlinear both by TIV and TV predictors, as the MSPE was lower for local prediction (low k) than for global prediction (high k), and was below its surrogate distribution. Moreover,

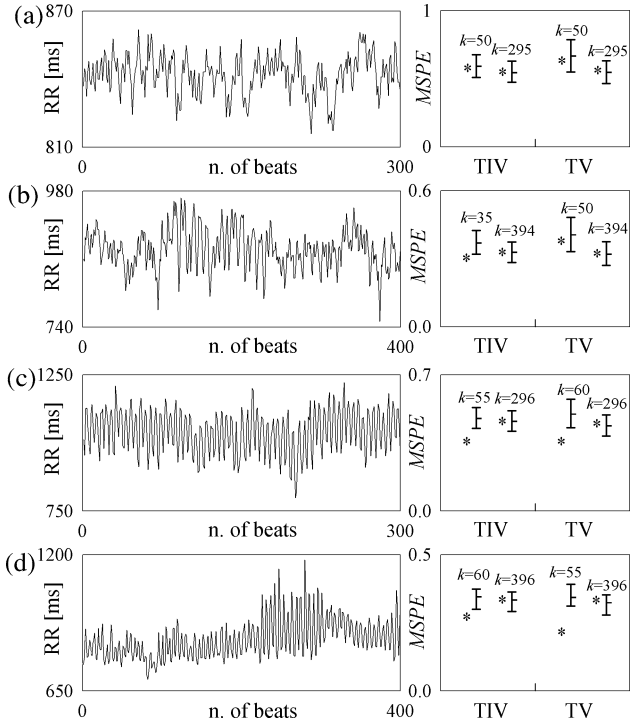

Fig. 3. RR interval variability series measured in four healthy subjects. (a) and (b) Spontaneous breathing. (c) and (d) Paced breathing. Asterisks in the right panels indicate the MSPE values obtained by TIV prediction (left) and TV prediction (right), either using a local predictor (low k) or a global linear predictor (high k), for which the number k of considered neighbors is indicated in the panels. MSPE distribution bars (expressed as 5th, 50th, and 95th percentiles) evaluated on 100 TIV surrogates (left) and 100 TV surrogates (right) are also indicated. Prediction was performed with $\tau = 1$ and with $P = 4, 5, 3, 3$ for the series (a)–(d).

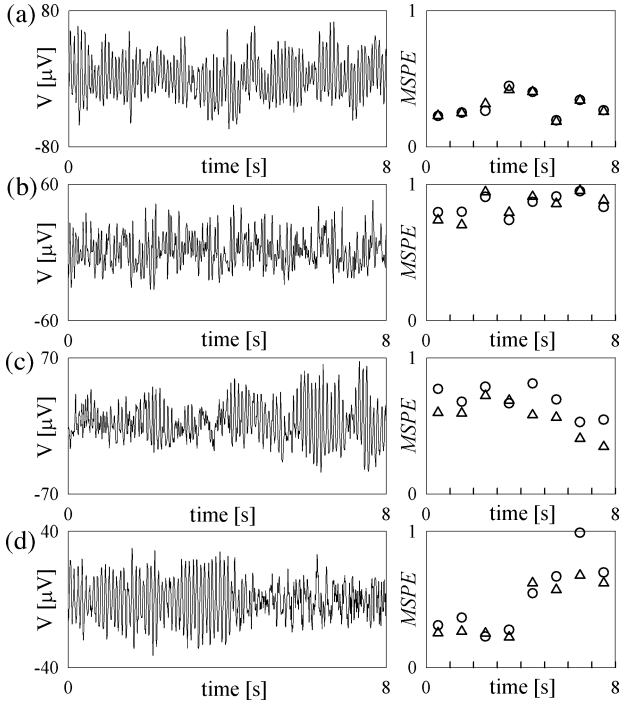

Fig. 4. EEG signals acquired in four healthy subjects. (a) and (c) Eyes-closed conditions. (b)–(d) Eyes-opened conditions. Right panels indicate the MSPE obtained by TIV prediction (circles) and TV prediction (triangles) within consecutive temporal windows of 1 s each. Prediction was performed with $\tau = 3, 3, 4, 3$ and with $P = 4, 5, 3, 2$ for the signals (a)–d), using the number of neighbors k that yielded the best prediction on the whole 8-s epoch.

the nonstationary transition of Fig. 3(d) was better captured by TV prediction ($M = 1$, Walsh function), as the MSPE was lower than that of TIV prediction ($M = 0$).

In the second application, we considered four EEG signals acquired in young healthy subjects from frontal head locations (standard 10–20 acquisition system, sampling rate = 128 Hz). The first two signals [see Fig. 4(a) and (b)] were judged by an expert reader as stationary eyes-closed and eyes-opened recordings. In these signals, the MSPE values obtained by TIV and TV prediction were comparable and were almost stable when evaluated over consecutive time windows of 1 s length. A larger predictability (lower MSPE), related to the presence of a dominant regular alpha rhythm, was measured during eyes closed. The signals of Fig. 4(c) and (d) were classified as showing a slow establishment and an abrupt interruption of alpha-EEG activity, respectively. In these signals, TV nonlinear prediction (with $M = 3$ Legendre and $M = 1$ Walsh basis functions, respectively) led to a lower MSPE than TIV prediction ($M = 0$). Moreover, by using TV prediction instead of TIV prediction, the time course of the MSPE index was better able to reflect both the expected slow increase of predictability of Fig. 4(c) and the expected subtle loss of predictability of Fig. 4(d).

V. Conclusion

The proposed TV nonlinear prediction method appears suitable to quantify the complexity of biomedical signals exhibiting nonlinear and/or nonstationary behaviors. As shown by the reported simulations, the use of a local linear predictor with small neighborhood sizes favors the accurate evaluation of complexity even in nonlinear time series. At the same time, the expansion of the TV AR coefficients onto a set of proper basis functions allows to evaluate complexity even in case of time-changing dynamics, as well as to track possible dynamic variations of the signal complexity. Moreover, the use of TV nonlinear prediction together with TV surrogates extends the applicability of the surrogate-based test for nonlinearity to biological signals, in which nonstationary behaviors are quite common. All these peculiar features make the proposed method eligible to describe the complex and nonstationary signals produced by a variety of biological systems. We reported instances of cardiovascular and brain signals, showing that TV nonlinear prediction is appropriate for HRV time series and EEG signals that are likely to exhibit significant nonlinear dynamics and/or TV complexity degrees.

References

[1] G. G. Berntson, J. T. Bigger Jr., D. L. Eckberg, P. Grossman, P. G. Kaufmann, M. Malik, H. N. Nagaraja, S. W. Porges, J. P. Saul, P. H. Stone, and M. W. Van Der Molen, "Heart rate variability: Origins, methods, and interpretive caveats," *Psychophysiology*, vol. 34, pp. 623–648, 1997.

[2] N. V. Thakor and S. Tong, "Advances in quantitative electroencephalogram analysis methods," *Annu. Rev. Biomed. Eng.*, vol. 6, pp. 453–495, 2004.

[3] A. M. Bianchi, L. Mainardi, E. Petrucci, M. G. Signorini, M. Mainardi, and S. Cerutti, "Time-variant power spectrum analysis for the detection of transient episodes in HRV signal," *IEEE Trans. Biomed. Eng.*, vol. 40, no. 2, pp. 136–144, Feb. 1993.

[4] M. Arnold, W. H. Miltner, H. Witte, R. Bauer, and C. Braun, "Adaptive AR modeling of nonstationary time series by means of Kalman filtering," *IEEE Trans. Biomed. Eng.*, vol. 45, no. 5, pp. 553–562, May 1998.

[5] P. Mansier, J. Clairambault, N. Charlotte, C. Medigue, C. Vermeiren, G. LePape, F. Carre, A. Gounaropoulou, and B. Swynghedauw, "Linear and non-linear analyses of heart rate variability: A minireview," *Cardiovasc. Res.*, vol. 31, pp. 371–379, 1996.

[6] C. J. Stam, "Nonlinear dynamical analysis of EEG and MEG: Review of an emerging field," *Clin. Neurophysiol.*, vol. 116, pp. 2266–2301, 2005.

[7] J. D. Farmer and J. J. Sidorowich, "Predicting chaotic time series," *Phys. Rev. Lett.*, vol. 59, pp. 845–848, 1987.

[8] R. Zou, H. Wang, and K. H. Chon, "A robust time-varying identification algorithm using basis functions," *Ann. Biomed. Eng.*, vol. 31, pp. 840–853, 2003.

[9] M. Casdagli, "Chaos and deterministic versus stochastic nonlinear modeling," *J. Roy. Stat. Soc. B*, vol. 54, pp. 308–328, 1991.

[10] J. Theiler, S. Eubank, A. Longtin, B. Galdrikian, and J. D. Farmer, "Testing for nonlinearity in time series: The method of surrogate data," *Physica D*, vol. 58, pp. 77–94, 1992.

[11] L. Faes, H. Zhao, K. H. Chon, and G. Nollo, "Time-varying surrogate data to assess nonlinearity in nonstationary time series: Application to heart rate variability," *IEEE Trans. Biomed. Eng.*, to be published.

[12] Y. Chen, G. Rangarajan, J. Feng, and M. Ding, "Analyzing multiple nonlinear time series with extended Granger causality," *Phys. Lett. A*, vol. 324, pp. 26–35, 2004.